

LAB 2: MEDICAL IMAGE SEGMENTATION

Image description

Atopic dermatitis (AD)



Figure 1. RGB image of atopic dermatitis on a hand (left) and homemade contour segmentation

Atopic dermatitis (AD), often referred to as eczema, is a chronic disease that causes inflammation, redness, and irritation of the skin. Until now, the clinical analysis of AD is based on subjective methods (SCORAD and EASI) [1]. As a consequence, currently, no methods enable to measure quantitatively the AD area. Thus, the idea is to segment the AD area in order to see its evolution in the time and according to change in the treatment.

Breast cancer ultrasound image

The second image used in this lab is a breast cancer malignant tumor acquired with ultrasound imaging and that comes from a larger Kaggle dataset [6].

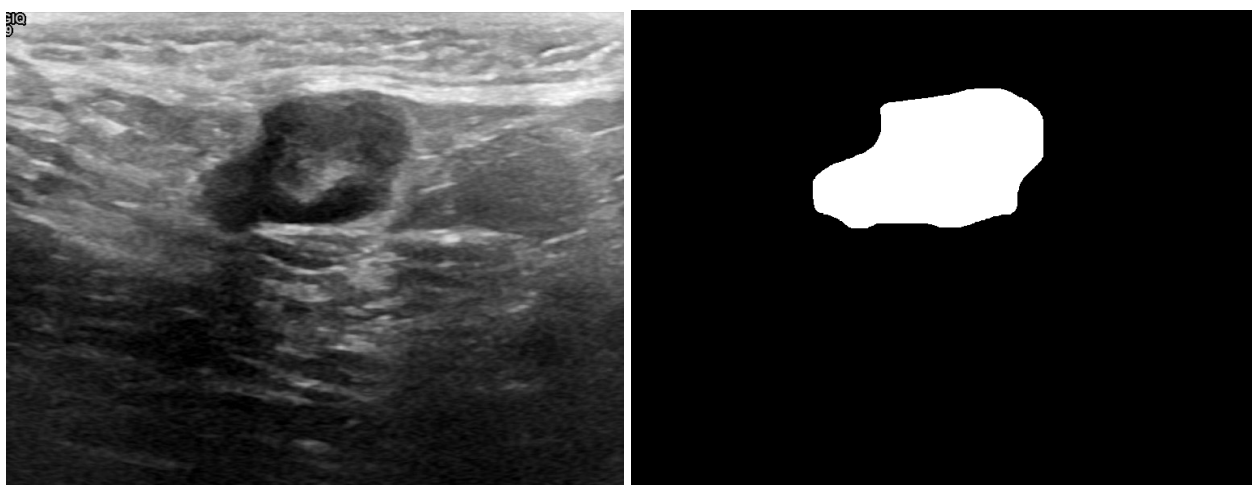


Figure 2. Breast cancer ultrasound image (left) and mask image (right)

The ultrasound image is really noisy and might have to be preprocessed. The mask image represents in white the region considered as the tumor and in black the rest. The idea of the segmentation for this image is to get as close as possible to the mask. We will use the mask as

ground truth in order to compare the results of our segmentation. As metrics, we will use Intersection over Union (IoU) and accuracy. The different metrics are defined following the next equations:

$$IoU = \frac{TP}{TP + FP + FN} \text{ and } Accuracy = \frac{TP + TN}{TP + TN + FP + FN}$$

PART 1: THRESHOLDING, REGION GROWING AND WATERSHED

Thresholding

AD RGB image

AD is hard to segment using the RGB image because of the color similarity between healthy and ill areas. An idea is to use the different channels of the RGB area (see Fig. 3).

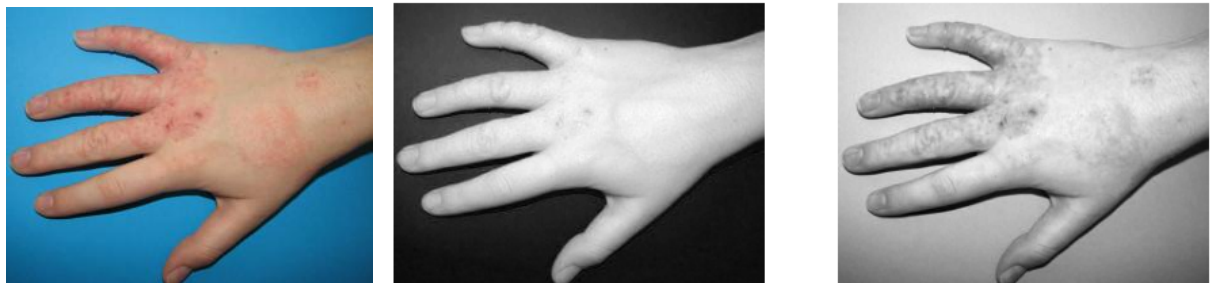


Figure 3. Visual comparison between RGB (left), red channel (center) and green channel (right) of the atopic dermatitis image

Firstly, we can see on Fig. 4 that the red channel histogram has different peaks which makes it easy to segment using thresholding. That enables us to first separate the hand from the background.

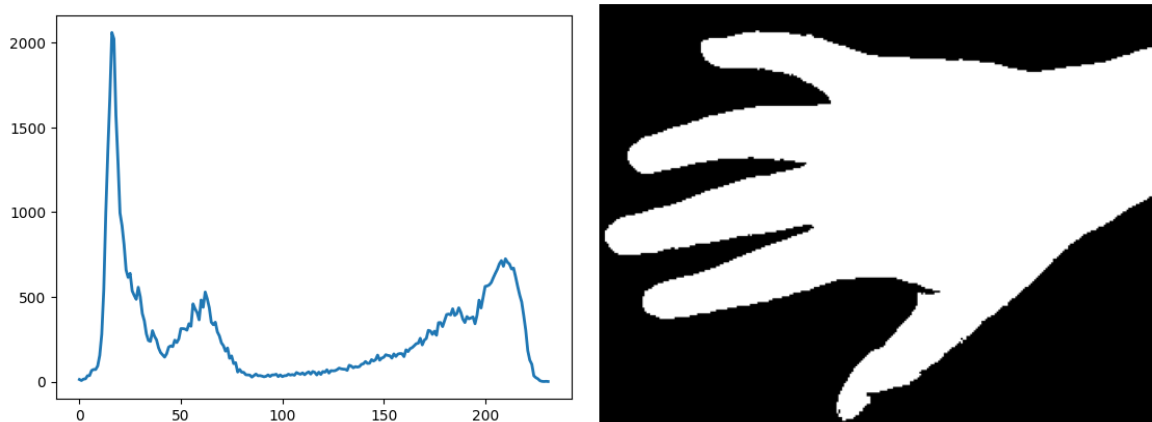


Figure 4. Red channel histogram (left) and result of the thresholding using otsu algorithm (right)

We can observe (Fig 5.) that the histogram has not well-separated peaks which makes it difficult to segment regions using thresholding. Indeed, the resulting image takes almost all the back of the end and does not really select the ill region.

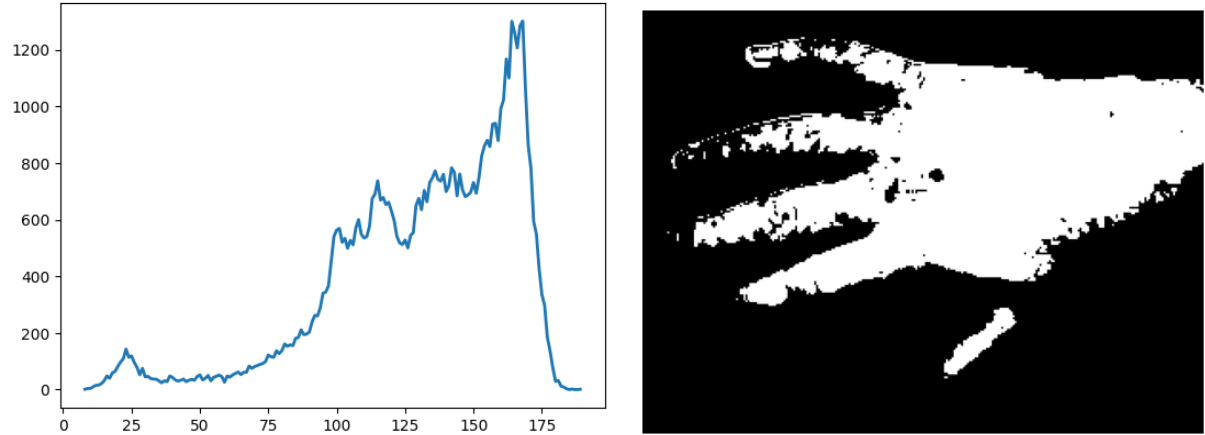


Figure 5. Green channel histogram (left) and result of the thresholding using multi-otsu algorithm (right)

Then, we decide to try histogram equalization and adaptive histogram modification on the green channel to see if we can have a histogram with well separated peaks. We can see in Fig. 6 that histogram equalization really seems to enhance the ill region.



Fig 6. Visual comparison of green channel (left), histogram equalization (center) and adaptive equalization (right) on dermatitis green channel

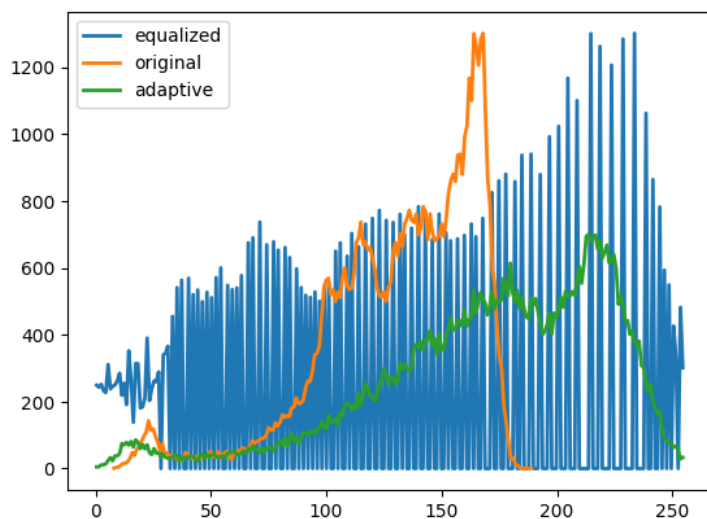


Fig 7. Comparison of green channel histogram before modification (orange), after equalization (blue) and after adaptive equalization (green)

We can see in Fig. 7 that the equalization enhances the contrast (broader distribution) but does not produce three clear peaks. As a consequence, it does not enable us to perform an outstanding segmentation using thresholding (see Fig. 8). We are still able to see the halo effect of the flash taking the picture.

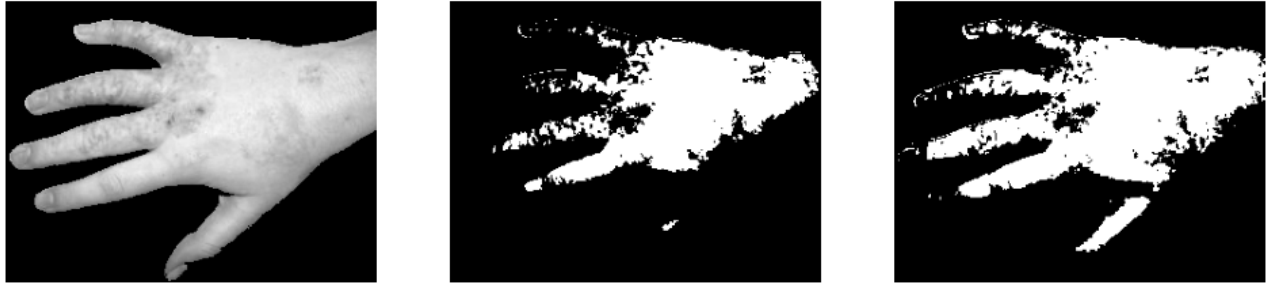


Figure 8. Visual comparison of green channel image (left), histogram equalization (center) and adaptive histogram equalization (right) thresholding using multi-otsu algorithm

Let's try another space color to enhance the contrast: the Lab space color. This color space is based on three channels, with "L" representing the lightness, "a" the green-magenta contrast and "b" the blue-yellow contrast. In [2], the authors use this space color to then segment the image using the k-means algorithm. We will try this technique in another section. First, we can observe (Fig. 9) that the histogram of the "a" channel has three well separated peaks and that the ill region seems brighter in the image.

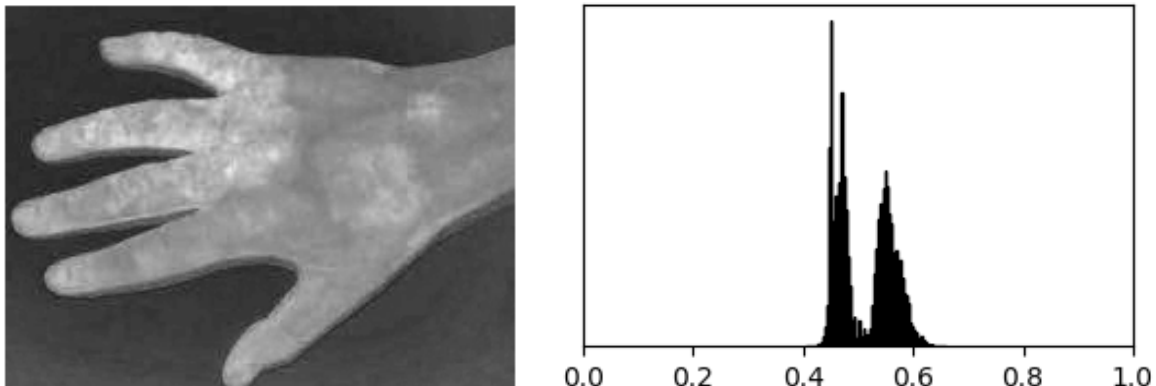


Figure 9. Visualization of "a" channel (left) and its histogram (right) from the AD hand image

As a consequence, we can use the multi-otsu thresholding algorithm in order to segment the image. Finally, we can see (Fig. 10) that the "a" channel enables us to get the best results. The thumb is still wrongly segmented as ill but the whole back of the hand is not anymore.



Figure 10. Visual comparison of “a” channel image thresholded with multi-otsu algorithm (left) and the original dermatitis image (right)

We can conclude that the “a” channel is the best color space to represent the AD lesions. The segmentation is quick, without any pre-processing need (histogram equalization etc) and allow to get all the ill regions and few true negative pixels.

Breast cancer ultrasound image

Firstly, we display the histogram of the original breast cancer ultrasound image to assess the potential of segmentation using thresholding (see Fig. 11). We can observe that one peak is clearly defined but a wide gray band is also visible. This will complicate our work.

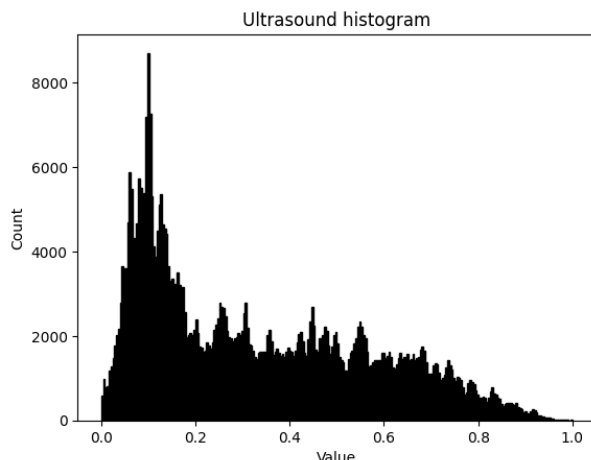


Figure 11. Visualization of the breast cancer ultrasound image histogram

Nevertheless, we try to use the Otsu algorithm to segment our image. As the histogram has not two clearly separated peaks, we segment the image by using a multi-Otsu algorithm in order to test different threshold values. Then, we either select the pixel values below the low threshold or between the low and high threshold (see Fig 12).

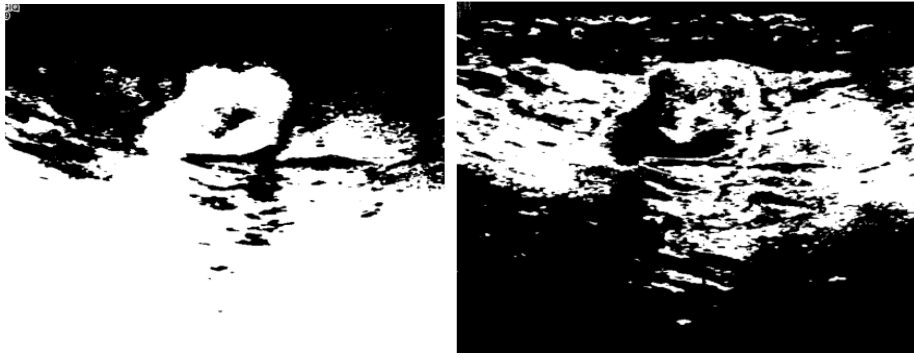


Figure 12. Visualization of otsu thresholding results on breast cancer ultrasound image using 3 classes selecting the pixel values situated under the smaller threshold (left) or the pixel values situated between the two thresholds (right)

As thresholding on the original image does not produce convenient results, we try to pre-process the ultrasound image using NLM and histogram equalization. However, we can see in Fig. 13 that it still does not allow us to get satisfying results.

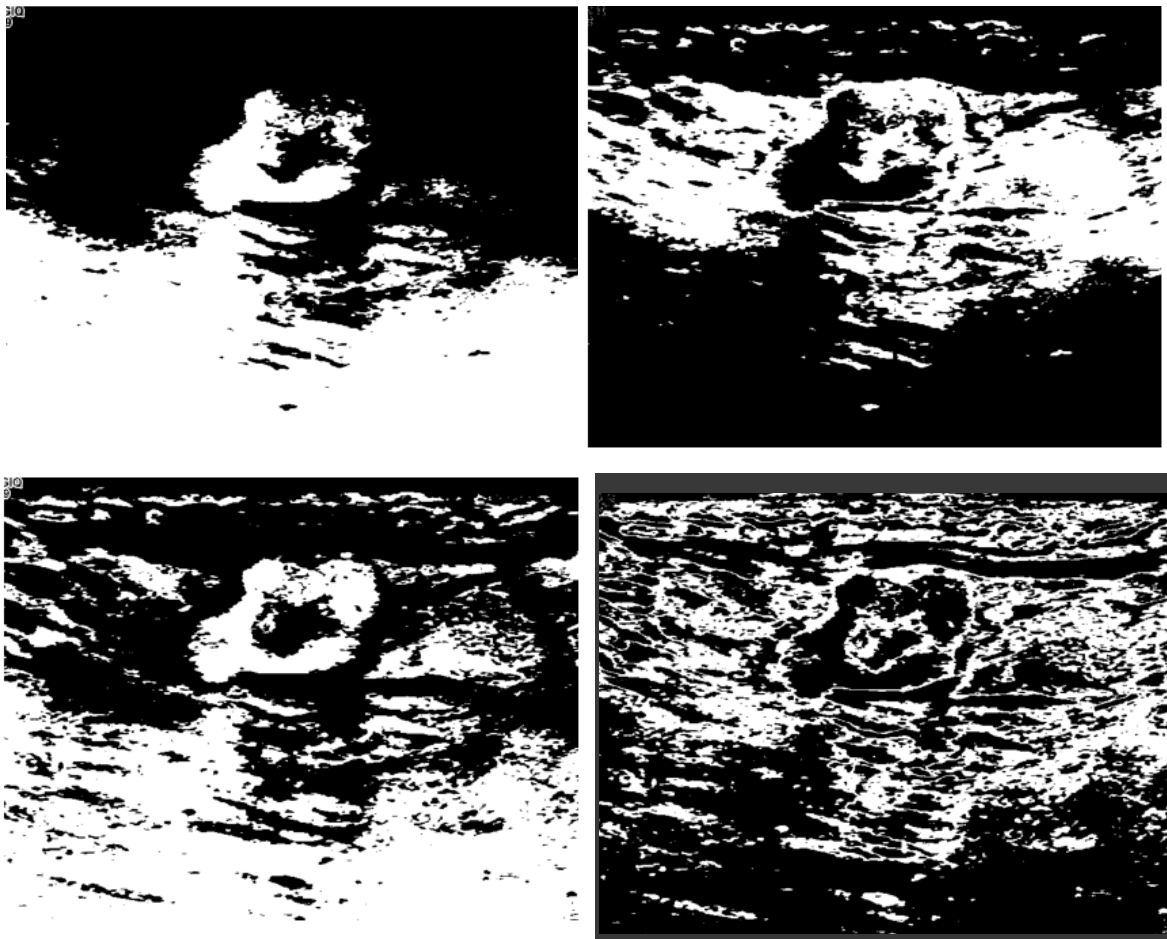


Figure 13. Visual comparison of 3 channels otsu thresholding results on breast cancer ultrasound image after fast NLM filtering, low threshold (up left), medium threshold (up right) and after histogram equalization, low threshold (down left), high threshold (down right)

At this point, we understand that the difficulty of the ultrasound image remains in the fact that the brightness is not homogeneous in the image. This is why denoising using NLM does not change anything and that histogram equalization just spreads the light differences in different parts of the

image. As a consequence, we intend to uniformate the light in the image using another technique. Indeed, if we use the low threshold, it will enable us to segment the tumor region but it will also select the low part of the image which has a similar intensity to the tumor. If we get to have the same brightness in the lower part of the image than in the higher part, we could efficiently segment the ultrasound image using the low thresholding. However, we do not want to increase the darkness in the high part of the image because in this region, the tumor is already well differentiated from the background. Thus, in order to reduce the darkness of the low part, we correct its histogram with a negative gamma transformation (see Fig. 14).

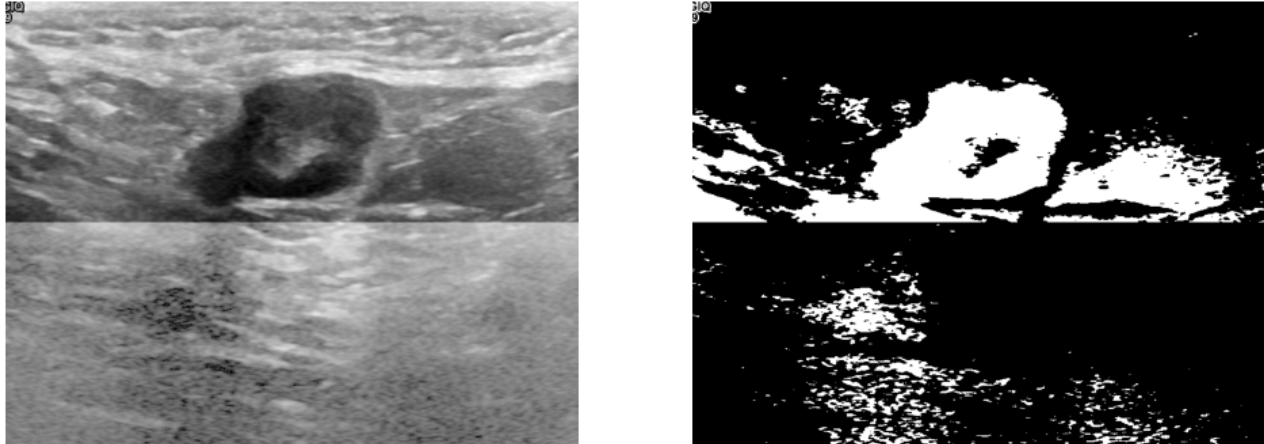


Figure 14. Visualization of breast cancer ultrasound image with low part enlightened using gamma histogram modification, $\gamma=0.3$ (left) and low thresholding using multi-otsu algorithm of 3 channels on the corrected image (right)

Finally, we can use morphological operations to remove the tiny points situated in the low part of the image (see Fig 15). The closing operation using a disk larger than the tiny points (10 pixels) enables us to improve the segmentation results (see Table 1).

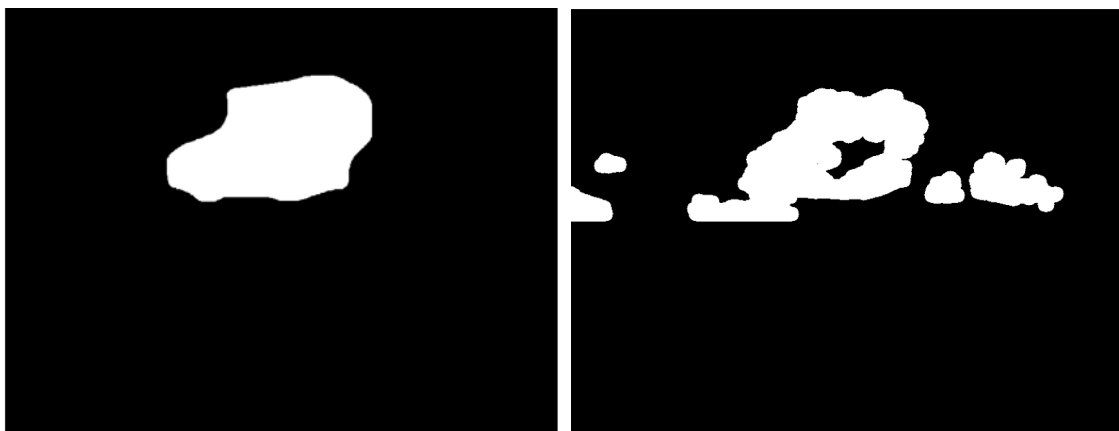


Figure 15. Visual comparison of brain cancer ultrasound mask image (left) and pre-processing of the thresholded image using 10 diameter disk closing

Pre/Post-processing	IoU	Accuracy
<i>Low band</i>	0,29	0,11
<i>Medium band</i>	0,4	0,19
<i>NLM + Low band</i>	0,29	0,11
<i>NLM + High band</i>	0,4	0,19
<i>Histogram equalization + Low band</i>	0,31	0,003
<i>Histogram equalization + High band</i>	0,35	0,008
<i>Low band + Gamma histogram correction ($\gamma=0.3$)</i>	0,61	0,17
<i>Low band + Gamma histogram correction ($\gamma=0.3$) + Closing (10 px disk)</i>	0,74	0,66

Table 1. Intersection over Union (IoU) and Accuracy values for Thresholding of the breast cancer ultrasound image according to different Pre/Post-processing methods.

Segmentation using thresholding is a hard task with an ultrasound image like this as the levels of intensity are not the same in all regions. It might be caused by the ultrasound depth or because of the difference in composition of the breast tissues. Interesting results are obtained by correcting the darkness in the lower part of the image.

Watershed

We discovered that an example of a watershed algorithm was available on the OpenCV website. It was shown to segment an image with coins that cannot be thresholded with classic segmentation. It is made in different steps:

- Estimation of the regions of interest with Otsu's threshold
- Noise removal with morphological opening on the thresholded image
- Dilatation of the image to expand the bright regions of the image representing the sure background area (area which we are sure they are not interesting)
- Distance transform operation which calculates the distance of each white pixel in the binary image to the closest black pixel and gives
- Threshold of the distance transform image to obtain the foreground (area which we are sure they are interesting).
- Subtraction of the unknown area that corresponds to the gray area between the white part of the background and the white part of the foreground by applying markers (“connectedcomponents” method from OpenCV is used to find the connected components in the sure foreground image)
- Apply Watershed Algorithm to Markers

We decided to use it for our 3 images, with some possibilities of modification.

AD RGB image

We first tried to perform the algorithm on the original image. We clearly see that the result is not a success. Indeed, the first thresholding and the distance transform image could not detect the region of interest.



Figure 16. AD image after watershed segmentation

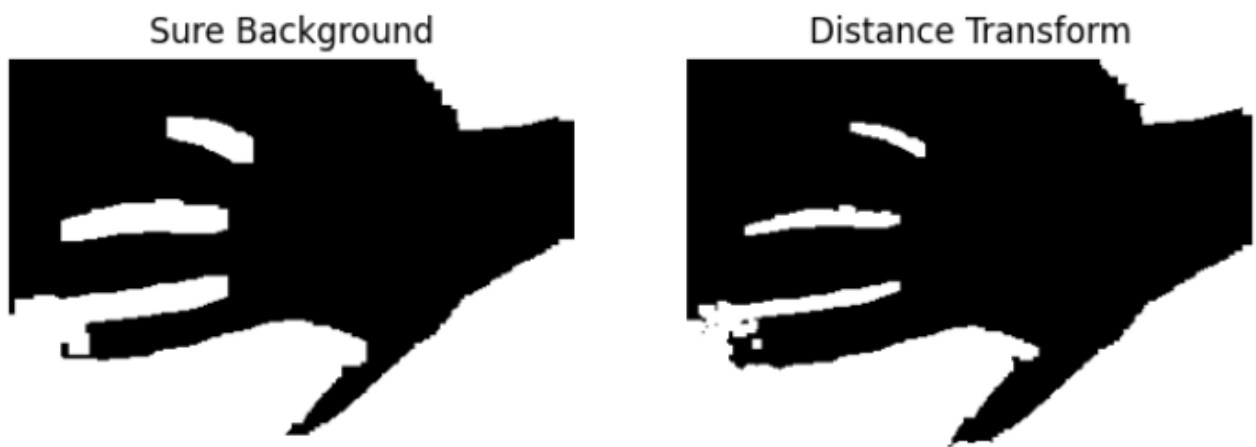


Figure 17. AD background and distance transform image.

To solve the problem, we will use the a_channel image thresholded with multi-otsu algorithm (see Figure 11) to realize the first threshold of the algorithm:

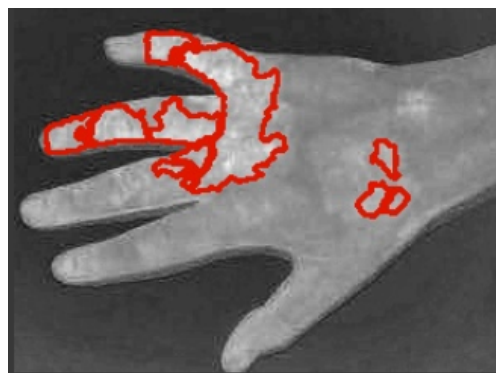


Figure 18. a_channel thresholded AD image after watershed segmentation

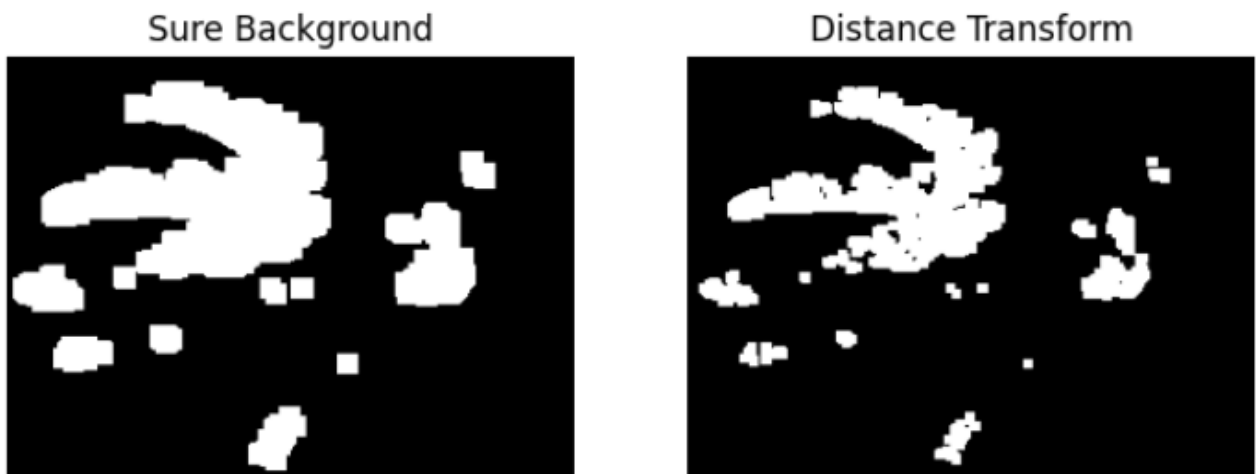


Figure 19. a_channel thresholded AD background and distance transform image.

The segmentation is satisfactory, but we would like to obtain continuous regions. To do so, we added a dilatation on the a_channel thresholded AD image after the noise removal. The result is much better:

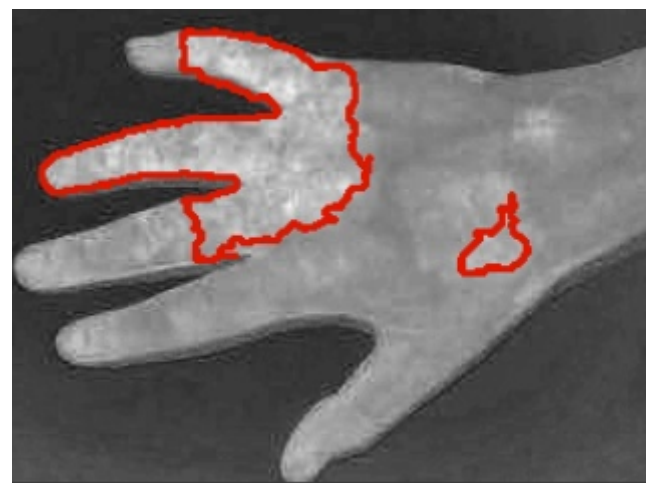


Figure 20. a_channel thresholded AD image after dilatation and watershed segmentation

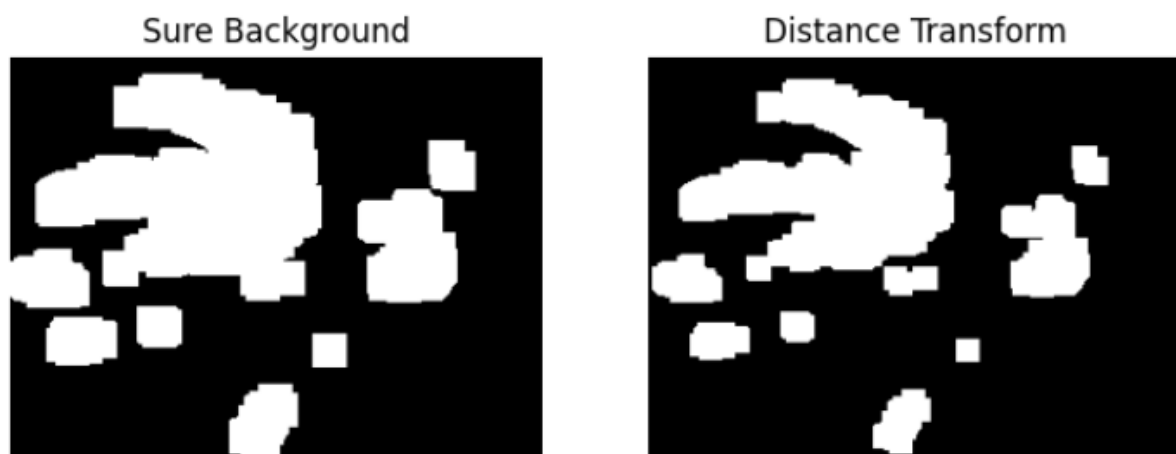


Figure 21. New a_channel thresholded AD background and distance transform image.

To improve the segmented image, post processing could have been realized such as morphological operation or smoothing and filtering. Experimentation of the different parameters for the distance transform could be useful to get better results.

Breast cancer ultrasound image

We first try to perform the watershed algorithm on the original image:

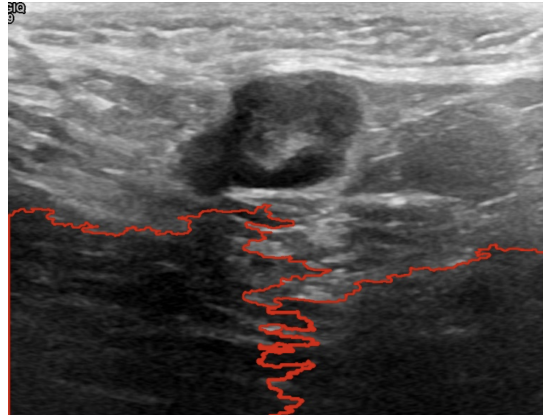


Figure 22. Breast cancer ultrasound image after the watershed algorithm

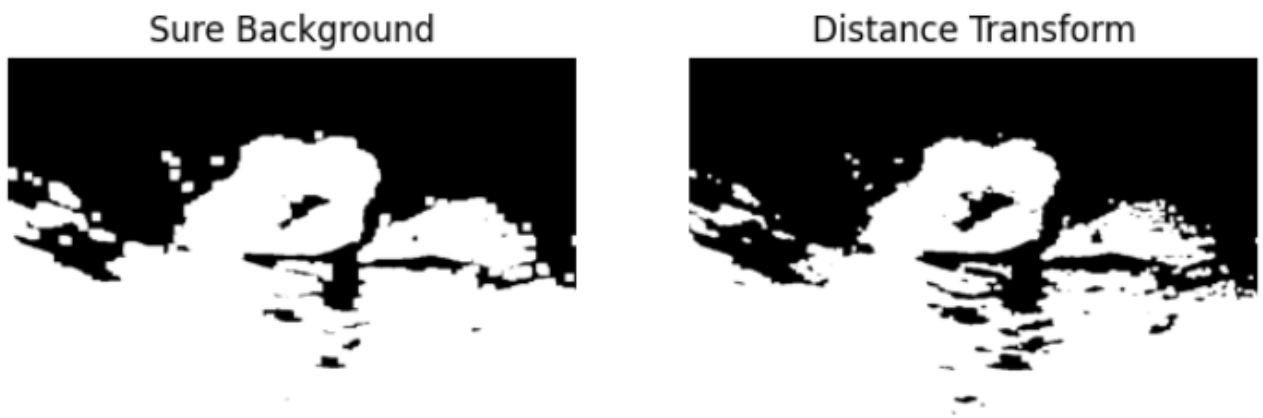


Figure 23. Breast cancer ultrasound background and distance transform image after the watershed algorithm. We clearly see that ROI is not well detected

As previously, the result is not satisfactory, it is even worse than for the AD image. It is due to the fact that the lower part of the image is dark, but also the lack of homogeneity of the image due to ultrasound penetration. Preprocessing has been tried by using Gaussian filter or adaptive histogram equalization, but the result is still the same.

Nonetheless, we tried to perform it on the ... image:

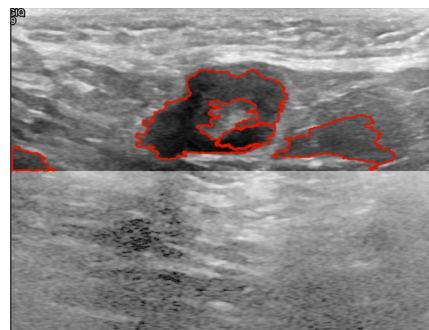


Figure 24. Breast cancer ultrasound corrected image (Figure 14) after the watershed algorithm

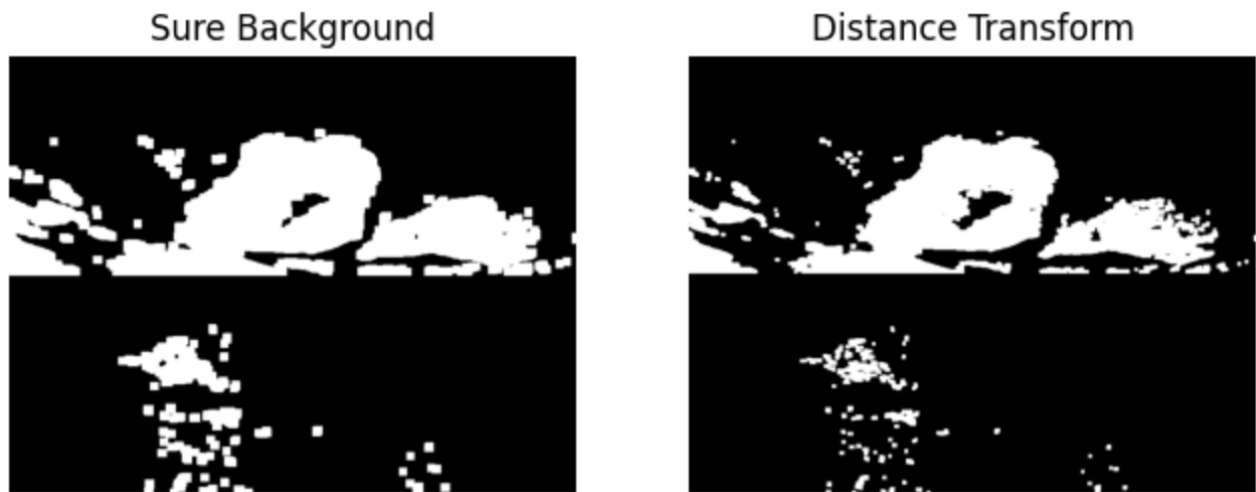


Figure 25.Breast cancer ultrasound corrected background and distance transform image after the watershed algorithm.

From the segmented image, we can easily obtain an black and white image where the region of interest is filled with white and the other part are black:

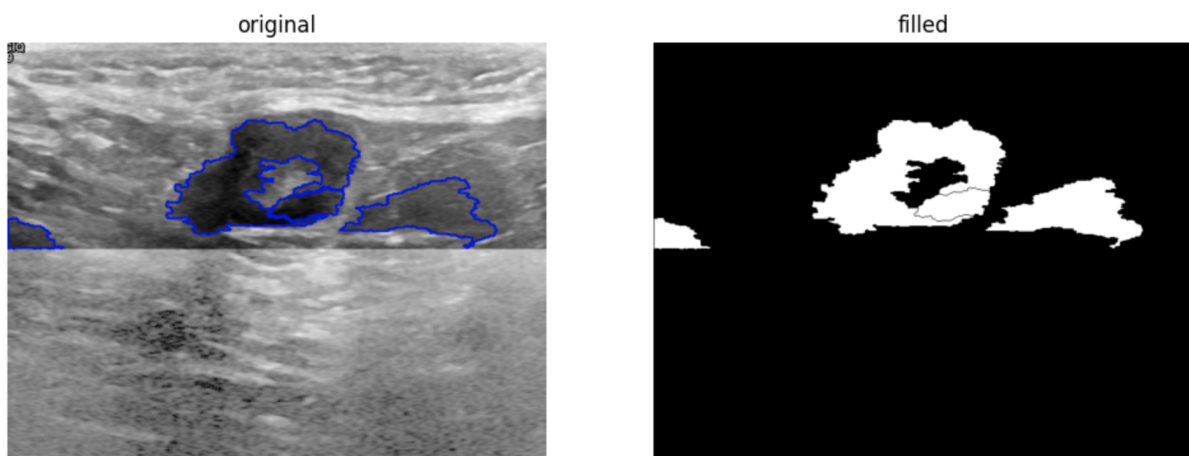


Figure 26.Breast cancer ultrasound corrected segmented with the watershed algorithm (left) and black and white image with ROI filled with blank (right)

We then compute Intersection over Union (IoU) and accuracy by comparing the filled image with the malignant_mask (Figure 15 left). We obtain $\text{IoU}: 0.7323817$ and $\text{Accuracy}: 0.664406779$. These results have been obtained without pre-processing. A closing or opening have been considered, but it would not have worked:

- Closing would have joined the bottom-right part of the tumor with the white zone a little further to the right
- Opening would have lost some parts of the tumor, maybe even half of the image.

Region growing

This algorithm is based on the idea to grow image regions from seeds (origin points) according to the similarity between pixels. In this part, we used an implementation of the region growing algorithm [5] that we adapted in order to have fixed seeds and not with on click selection as it was implemented.

AD RGB image

This time, we try the region growing algorithm on our images. This algorithm is based on the idea to grow regions from seeds according to the similarity between pixels. Thus, we need to define seeds in the image (see Fig. 27)

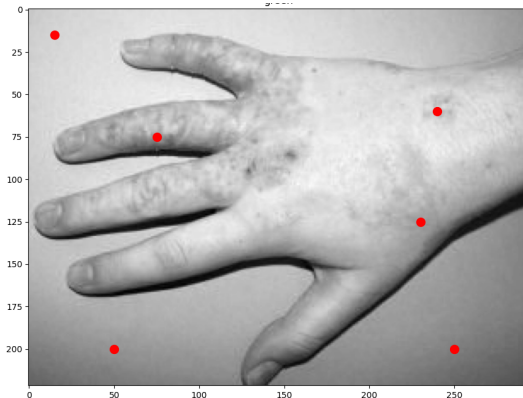


Figure 27. Visualization of the seeds used to apply the region growing algorithm on the AD image

Then, we first test this algorithm on the RGB image, using different thresholding values (see Fig. 28). The thresholding value is the limit between the intensity of two pixels considered as belonging to the same region. We can observe that a too large threshold value will cause the region to grow too much (the white region in this image).

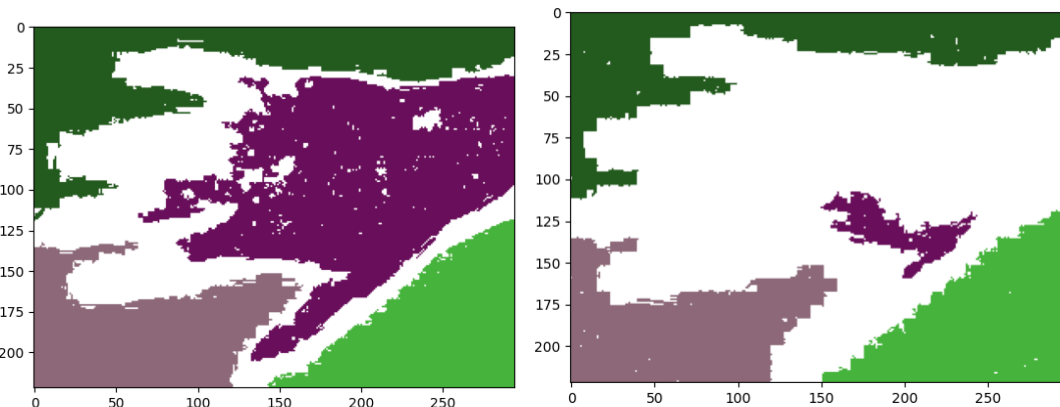


Figure 28. Comparison of region growing results on RGB image with threshold=5(left) and threshold=3 (right)

As the region growing algorithm does not produce sufficiently good results on the RGB image, we decide to use different color space changements and make some pre-processing (see Fig. 29). As we saw in the previous sections, the green or saturation channel enables us to enhance the ill region and the adaptive equalization to provide a more contrasted image.



Figure 29. Visualization of region growing results on normal green channel image with threshold=3 (left), saturation channel image with threshold=3 (center) and saturation channel with adaptive equalization and threshold=10 (right)

Finally, we test the region growing algorithm on the “a” channel of the Lab color space (see Fig. 30).

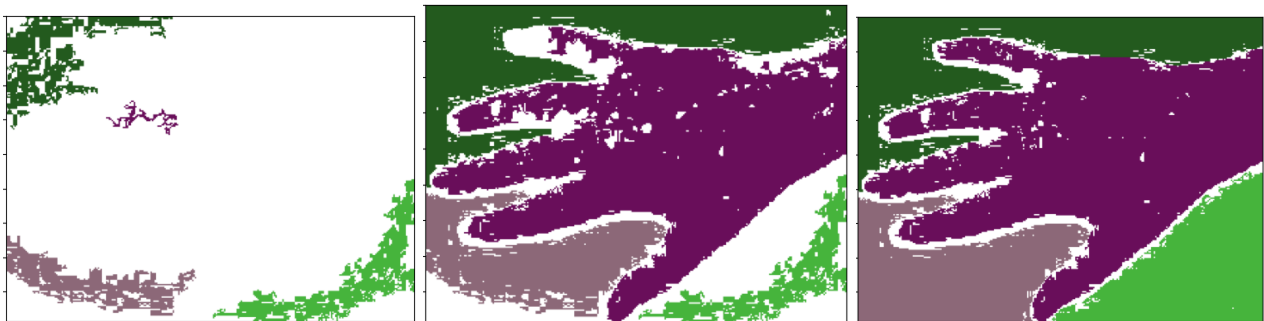


Figure 30. Visual comparison of region growing results on “a” channel of dermatitis image with threshold=6 (left), 7 (center) and 10 (right)

We can conclude that the region growing algorithm is not well suited for the AD image. indeed, the homogeneity condition is highly dependent of the intensity threshold. Sometimes, it “spreads too much” in some regions compared to others. As an example of this, with two close intensity thresholds, the RGB image does not produce good results, one having an ill region under-spread and the other with an over-spread ill region. Unlike with the thresholding, the “a” channel of the Lab color space does not improve the results. Actually, this is the green channel image that produces the best results with the region growing algorithm by detecting all the ill regions but unfortunately also the hand contour.

Breast cancer ultrasound image

As for the last image, the algorithm needs its own seeds. We decided to use only one for the breast cancer ultrasound image (see Fig.).



Figure 31. Visualization of the seed use in the region growing algorithm for the breast cancer ultrasound image

Firstly, we run the region growing algorithm on the original ultrasound image.

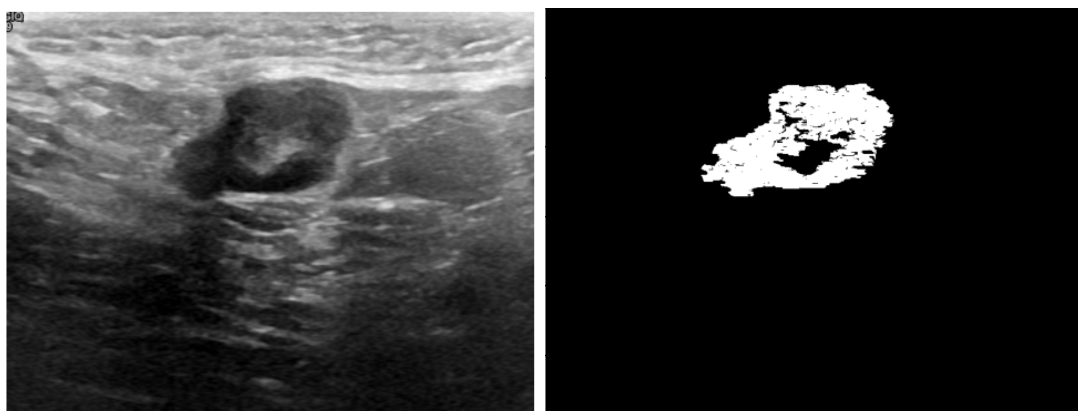


Figure 32. Visual comparison of the original breast cancer ultrasound image and the results of region growing segmentation with threshold=4

Then, as the ultrasound image is really noisy, we intend to do some pre-processing in order to improve the results of the region growing algorithm.



Figure 33. Visual comparison of region growing results on breast cancer ultrasound image with adaptive histogram equalization (left), fast Non-Local Means (NLM) (center) and adaptive histogram equalization on NLM denoise image (right)

As the biggest part of the mask which is not segmented is the center of the tumor, we can use post-processing to improve the results (see Table ...). Closing using a 20 pixels disk is the method chosen here (see Fig).



Figure 34. Visual comparison of mask (left) and region growing image filled by closing morphological operation(right)

Pre/Post-processing	IoU	Accuracy
/	0,82	0,7
NLM	0,76	0,7
Histogram equalization	0,7	0,68
NLM+Histogram equalization	0,78	0,7
Closing	0,9	0,7

Table 2. Intersection over Union (IoU) and Accuracy values for Region Growing of the breast cancer ultrasound image according to different Pre/Post-processing methods.

As a conclusion, the region growing algorithm works pretty well on the breast cancer ultrasound image. Indeed, as it spreads from a seed and does not merge regions if the homogeneity criterion is not met, the low part of the ultrasound image is not detected. The only default is that the ROI has to be detected first in order to put the seed in. Moreover, if the seed would have been in the brighter region of the tumor, the algorithm would not have worked as well.

PART 2: ACTIVE CONTOURS

The Snake algorithm is a contour-based algorithm that deforms a shape (the snake) in order to fit its constraints [7]. Those constraints are based on the minimization of the energy representing the smoothness and the continuity of the contour. The process relies on different steps. First a gaussian filter has to be applied in order to smooth the input image. Then, we need to select a shape that fits approximately the ill region of our image. Finally, we apply the snake algorithm using the function that can be found in [8]. We will see in this section how it allows us to detect the ill region in our image.

AD RGB image

First of all, we realize the smoothing of the original AD image with a gaussian filter ($\sigma=1$). Then, we create an ellipse shape for which coordinates of the center have been determined visually. Finally, we perform the snake algorithm:

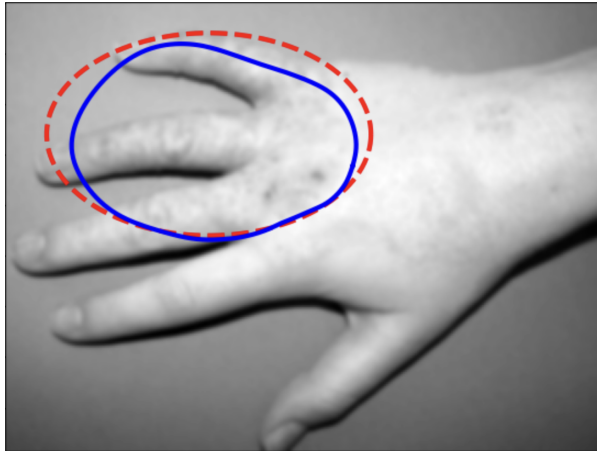


Fig 35. Visual comparison of snake algorithm results (blue) on the original AD image with a ellipse with center (65,100), semi-major axis 80px, and semi-small axis 50px (in red)

We can clearly see that the result is not satisfactory. It is mainly due to the fact that the shape that is used to realize the snake segmentation of the hand is too difficult to represent as it has to correspond to the region of interest.

The same process has been realized on the a_channel image:

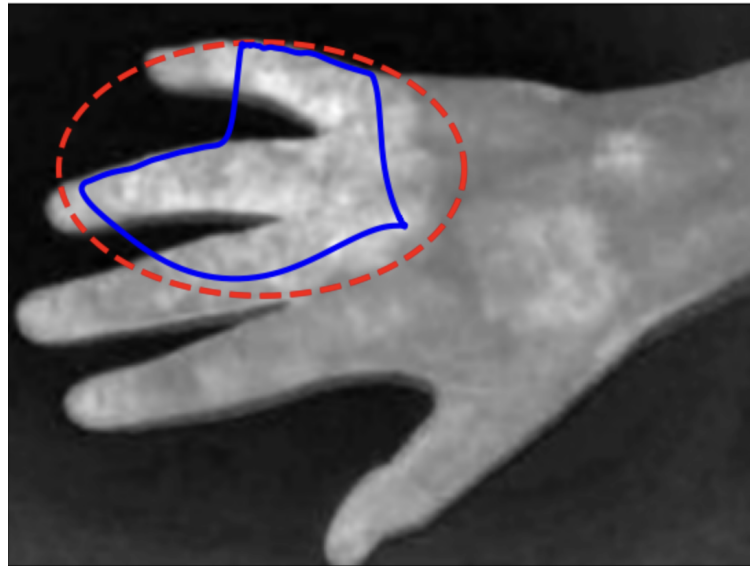


Fig 36. Visual comparison of snake algorithm results (blue) on the a_channel AD image with a ellipse with center (65,100), semi-major axis 80px, and semi-small axis 50px (in red)

The result is significantly better, thanks to the contrast highlighted by the a_channel image, but it is still not satisfactory. The problem of choosing a shape that corresponds to the ROI of the AD is still present. Maybe a rectangle would be better.

Breast cancer ultrasound image

Firstly, we perform gaussian filtering to smooth the image ($\sigma=3$). Then, we select a shape (the snake) to limit the region of research. Here, we decided to use a circle (or an ellipse) and not a rectangle because of the circular aspect that breast cancer tumors have. As it can be seen in Fig. 37, the snake algorithm provides highly different results according to the snake and the parameters chosen. However, it seems that using an elliptical shape allows to improve the performance of the segmentation (see Table 3).

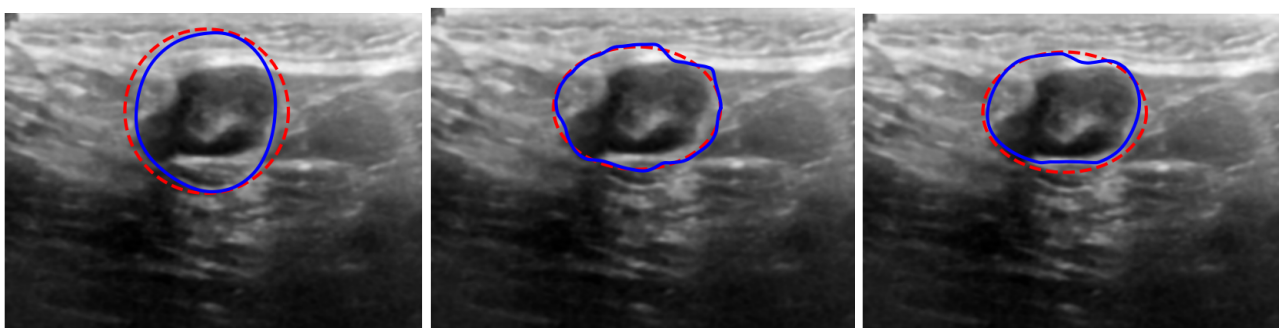


Figure 37. Visual comparison of snake algorithm results (blue) on breast cancer ultrasound image using a circle shape (red) of 75px diameter (left), a 75x55px diameter ellipse with documentation parameters (center) and the same ellipse with modified parameters

Pre/Post-processing	IoU	Accuracy
circle	0,74	0,51
ellipse, doc parameters	0,82	0,62
ellipse, manual tuning	0,85	0,67
ellipse, best automatic tuning	0,87	0,67

Table 3. Intersection over Union (IoU) and Accuracy values for Active Contour of the breast cancer ultrasound image according to different Pre/Post-processing methods.

Moreover, there are at least five parameters that can be tuned in the snake algorithm implementation proposed by skimage. As a consequence, we decided to perform an automatic parameter search based on the maximization of the IoU and accuracy (see Table 4). Those metrics are computed by filling the snake contour and comparing it to the mask reference.

alpha	beta	gamma	w_line	w_edge	sigma	iou	acc
0.010	20.0	0.005	0.5	1.0	3.0	0.866565	0.666102
0.015	10.0	0.005	0.5	1.0	3.0	0.862831	0.659322
0.010	10.0	0.005	0.5	1.0	3.0	0.861155	0.659322
0.020	10.0	0.010	0.5	1.0	3.0	0.859711	0.657627
0.020	10.0	0.005	0.5	1.0	3.0	0.859015	0.659322

Table 4. Best parameter configurations and their IoU and accuracy (acc) metrics in the parameter search on the snake algorithm with breast cancer ultrasound image

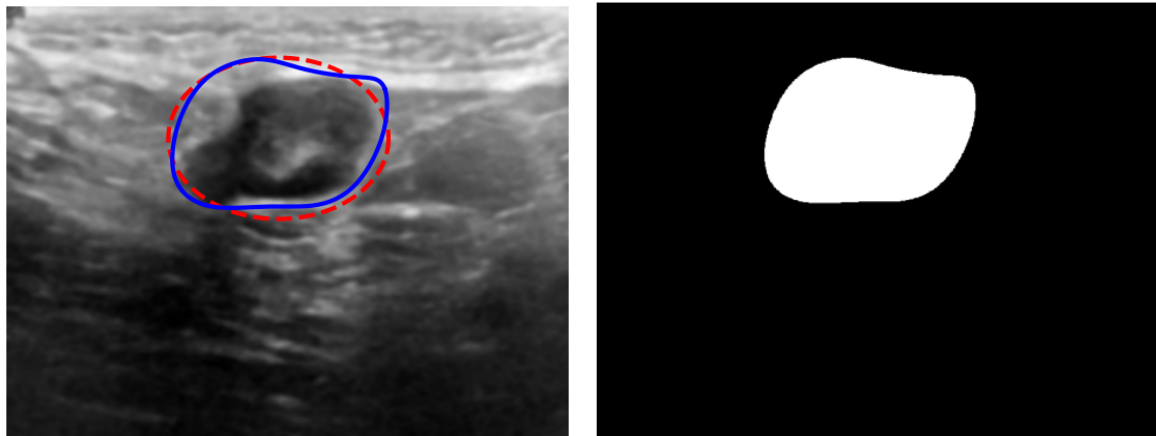


Figure 38. Visualization of the best parameter configuration results using snake algorithm on breast cancer ultrasound image, contour is in blue and initialization snake is in red (left), filled image (right)

PART 3: K-MEANS CLUSTERING

After the Lab color space transformation, another approach used in [1] is the k-means algorithm. With this method, they achieved increased results than with any other segmentation method. AS a consequence, we decided to test this method on our images.

AD RGB image

We first decided to test the k-means algorithm on the green channel of the RGB image (see Fig. 39).



Figure 39. Visualization of green channel of rgb AD image (left), k-means algorithm results on green channel with $k=3$ (center) and the selected label (right)

Then, we chose to compare it to the method using the “a” channel which proved its worth in the last sections. Indeed, the Lab space color allows us to get a better segmentation by avoiding the flash effect of the green channel (see Fig 40). As a consequence, we get the full ill region but also the thumb as in the region growing algorithm.



Figure 40. Visualization of “a” channel of Lab color space dermatitis image (left), k-means algorithm results on “a” channel with $k=3$ (center) and the selected label (right)

To conclude, the k-means works pretty well on the “a” channel as described in [1]. Indeed, all the ill regions are included in the segmentation and the thumb area is not that present.

K-means for breast cancer ultrasound image

As the K-means algorithm worked well on the AD image, we tried it on the breast cancer ultrasound image to see if this approach is well suited for noisy images too. Firstly, we computed the k-means algorithm on the original image (see Fig. 41)

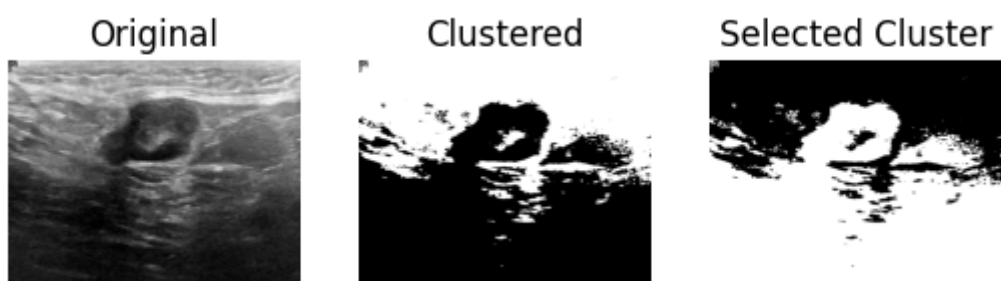


Figure 41. Visual comparison of original breast cancer ultrasound image (left), k-means results using k=2 on the original image (center) and the inverted k-means result (right)

As the original image has a similar intensity in the lower part than in the tumor, the k-means algorithm cannot converge to a good solution. Then, we can use the corrected image created previously for the segmentation using thresholding. We can observe (Fig. 42) that this time the correction does not enable to produce such better results (see Table 5).

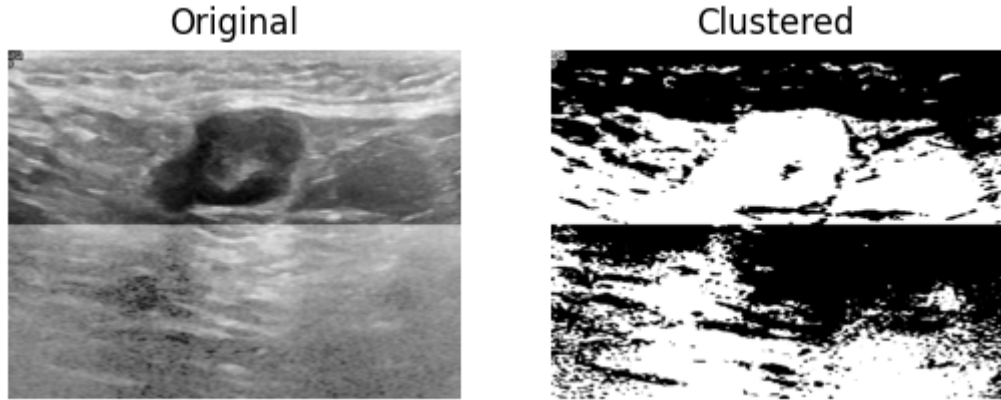


Figure 42. Visualization of breast cancer ultrasound image with low part enlightened using gamma histogram modification, $\gamma=0.3$ (left) and k-means results using k=2 on the corrected image (right)

As it worked for the thresholding, we decided to increase the number of classes used in the k-means algorithm. We can observe Fig. 43 that augmenting k enables us to reduce the number of pixels selected. As a result, it also allows us to improve the performance of the segmentation (see Table 5).

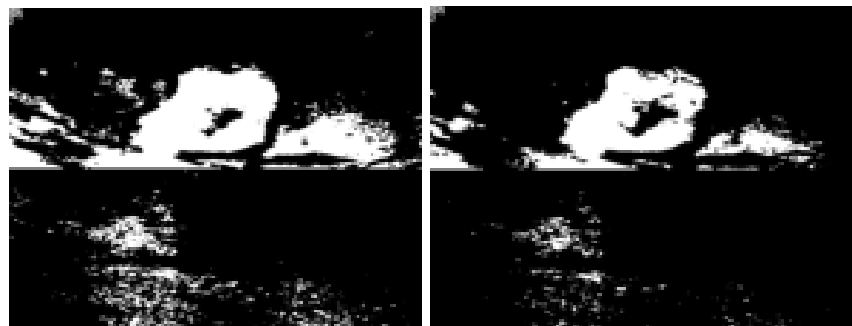


Figure 43. Visual comparison of k-means algorithm results on corrected breast cancer ultrasound image with k=3 (left) and k=5 (right)

Pre/Post-proc essing	IoU	Accuracy
/	0,25	0,11
<i>Low band + Gamma histogram correction ($\gamma=0.3$) , k=2</i>	0,35	0,02
<i>Low band + Gamma histogram correction ($\gamma=0.3$) , k=3</i>	0,61	0,17
<i>Low band + Gamma histogram correction ($\gamma=0.3$) , k=5</i>	0,69	0,25

Table 5. Intersection over Union (IoU) and Accuracy values for K-Means of the breast cancer ultrasound image according to different Pre/Post-processing methods.

As we can observe in this section, the k-means algorithm has low results with the original image. Enhancing the dark part of the image does produce better IoU and accuracy but which are not sufficient compared to other techniques.

CONCLUSION

To conclude, all these segmentation methods are interesting. They have many advantages and drawbacks, but they all have their specific use according to the image that should be segmented. The choice of segmentation method depends on the contrast between structures in the image, the distribution of ill regions in space (alone, separated), and the available resources for parameter tuning and processing time. Some methods work better for certain scenarios, while others may be more versatile but require careful setup. Researchers and practitioners often use a combination of these techniques to achieve optimal results in complex image segmentation tasks.

For the atopic dermatitis image, it is clear that the thresholding and the k-means algorithm with 3 classes on the “a” channel of the Lab color space produce the best results. Region growing is not able to produce interesting results because of the similarity of pixel intensity between ill and healthy regions. Watershed and active contours methods are not quite accurate due to the difficult edge shapes that have the AD image.

For the breast cancer ultrasound image, we observe that the best segmentation method is the region growing. It is due to the fact that the region growing algorithm continues to perform until the homogeneity condition is fully satisfied, consisting in staying in the tumor. Moreover, even if the snake method presents high values of Intersection over Union, the region growing method presents best values of Intersection over Union and Accuracy compared to the other segmentation method. It is possible that the Otsu algorithm is not optimum for ultrasound imaging where histograms do not usually present a bimodal shape. For example, in [4], the authors optimize the Otsu function using the Jaya algorithm.

<https://www.sciencedirect.com/science/article/pii/S1877050919306799/pdf?md5=10b121e1e8809ac99353885b35493e56&pid=1-s2.0-S1877050919306799-main.pdf>

References

- [1] Fishbein, Anna & Silverberg, Jonathan & Wilson, Eve & Ong, Peck. (2019). Update on Atopic Dermatitis: Diagnosis, Severity Assessment, and Treatment Selection. *The Journal of Allergy and Clinical Immunology: In Practice*. 8. 10.1016/j.jaip.2019.06.044.
- [2] Alam, Md & Munia, Tamanna Tabassum Khan & Tavakolian, Kouhyar & Vasefi, Fartash & MacKinnon, Nicholas & Fazel-Rezai, Reza. (2016). Automatic detection and severity measurement of eczema using image processing. Conference proceedings: ... Annual International Conference of the IEEE Engineering in Medicine and Biology Society. IEEE Engineering in Medicine and Biology Society. Conference. 2016. 1365-1368. 10.1109/EMBC.2016.7590961.
- [3] Open Source Computer Vision: Image Segmentation with watershed algorithm:
https://docs.opencv.org/4.x/d3/db4/tutorial_py_watershed.html
- [4] Rajinikanth, Venkatesan & Dey, Nilanjan & Kumar, Rajesh & Panneerselvam, John & Raja, N.. (2019). Fetal Head Periphery Extraction from Ultrasound Image using Jaya Algorithm and Chan-Vese Segmentation.
- [5] Region growing segmentation algorithm using python
<https://github.com/Spinkoo/Region-Growing>
- [6] Al-Dhabyani W, Gomaa M, Khaled H, Fahmy A. Dataset of breast ultrasound images. *Data in Brief*. 2020 Feb;28:104863. DOI: 10.1016/j.dib.2019.104863.
<https://www.kaggle.com/datasets/aryashah2k/breast-ultrasound-images-dataset>
- [7] Kass, M.; Witkin, A.; Terzopoulos, D. “Snakes: Active contour models”. *International Journal of Computer Vision* 1 (4): 321 (1988). DOI:10.1007/BF00133570
- [8] Skimage snake algorithm implementation
https://scikit-image.org/docs/stable/api/skimage.segmentation.html#skimage.segmentation.active_contour

Work distribution

Florent TACHENNE: 60% (Thresholding, region growing, active contours and k-means)
Stavros KOSTAS: 10% (Thresholding)

Victor POUSSAIN: 30% (Watershed and active contours)